Indoor Air 1998; 8: 113–122
Printed in Denmark. All rights reserved

Copyright © Munksgaard 1998
INDOOR AIR
ISSN 0905-6947

Modelling of the Indoor Environment – Particle Dispersion and Deposition

STURE HOLMBERG[1,2] AND YUGUO LI[3]

Abstract A three-dimensional drift-flux model for particle movements in turbulent airflows in buildings is presented. The interaction between the carrier air and the particles has been treated as a one-way coupling, assuming the effect of particles on air turbulence is negligible due to low solid loadings and comparatively small particle settling velocities. Turbulence effects are modelled with a standard κ-ε model. Wall functions are applied at near-wall grid points. Aerosol measurements carried out under turbulent room flow conditions are used to validate the numerical calculations. Several particle size distributions are considered in the simulations. The model is then applied to mixed flow conditions in a room, as well as to homogeneous air supply conditions around a human body. The flow fields and particle distributions are analysed. Close to a standing person, the particle distribution pattern from a downstream point source is strongly dependent on the ventilation air supply rate. This has been confirmed by experiments reported in the literature.

Key words Numerical simulations; Drift-flux models; Indoor aerosols; Particle dispersion; Particle deposition; Ventilation

Received 23 April 1997. Accepted for publication 14 November 1997.
© Indoor Air (1998)

Introduction

At workplaces, in residential buildings and in other indoor environments, people are continuously exposed to different particulate pollutants. Both in the airborne form and when deposited on surfaces these pollutants can be harmful, and better tools for predicting particle dispersion and deposition, as well as more knowledge regarding exposure control should be developed. The modern work environment and the way of working have changed with the technical development in our society. A better indoor air quality has been aimed at and this is today an important measure of our development. The environmental requirements are higher today than they were when the traditional industrial ventilation concepts were developed. Workplaces have become cleaner and more people than before are used to working in office environments. The health and well-being of people has, however, been improved only marginally. Many new chemicals and dangerous substances, originating from indoor and outdoor sources, are still present in the air. This is evidenced by the increasing number of "sick-building"-related diseases. It is therefore important for us to be able to predict the contaminant movements in air and to find out how to minimize the total exposures. The movements of passive contaminants, i.e. gases, are already quite well understood from an engineer's point of view and is not the topic of this investigation. The focus here is on non-passive (indoor) particles that do not exactly follow the main airstream movements of the room. The modelling aspects considered include particle movements, particle dispersion and particle settling on surfaces.

Characteristics of Particles in Indoor Environments

To be able to solve the indoor environmental health and contamination problems, it is important to identify the potential sources of indoor particles. The sizes and typical particle concentrations can then be determined. Owen et al. (1992) classify particles (aerosols) into the following six groups: bioaerosols (plant and animal), mineral, combustion, home/personal care and radioactive aerosols. Bioaerosols contain particles of living origin. These types of particle present a special hazard as allergens. Particles belonging to this group may be very small and remain airborne for long periods, or quite large and remain in the air only for short periods.

---

[1] Work Organisation and Technology, National Institute for Working Life, S-171 84 Solna, Sweden, [2] Department of Built Environment, Royal Institute of Technology (KTH), Box 88, S-801 02 Gävle, Sweden (from January 1998), [3] Advanced Thermo-Fluids Technologies Laboratory, CSIRO, Building, Construction and Engineering, Highett, Victoria, Australia

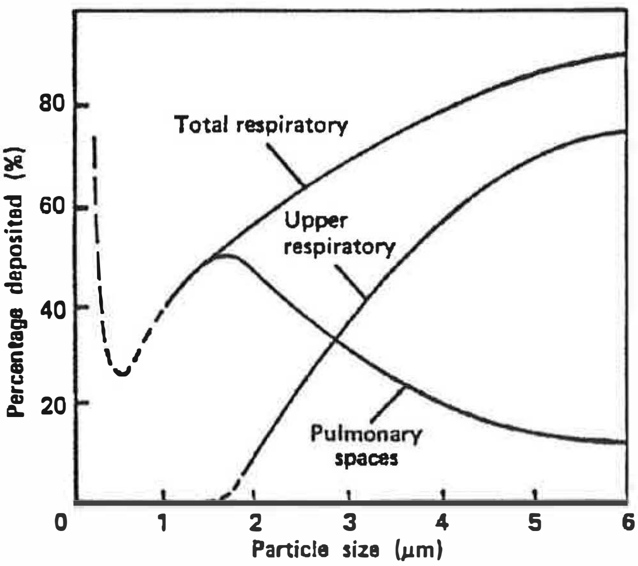

Fig. 1 Particle deposition (unit density spheres) in the respiratory system (Wickham, 1992)

Mineral aerosols are non-organic and do not present the infection potential of the previous group but may be carcinogenic or mutagenic. Mineral fibres are used extensively in building materials. They are manufactured from glass, rocks, ceramics, etc. Most of the combustion aerosols are in the respirable range and need to be considered when designing an air quality control system. Tobacco smoke is a well-known complex problem substance in this group. Also, there is concern that small particles from motor vehicles, especially diesel exhaust, can contribute to the development of certain diseases, e.g. asthma. Chemicals, including sprays, used and generated in homes and offices belong to the last group. They often present a health hazard by their chemical nature and their presence in the circulating indoor airstream. Radioactive particles, i.e. radon progeny, are unwelcome elements in the indoor environment. They are ultra small and may attach to larger particles. An efficient ventilation system can, in many cases, be useful in controlling exposure rates.

The size distribution of indoor dust will vary with location; there appears, however, to be a pattern. The size of dust particles is significant when assessing their likely deposition in the airways. Particles greater than 3 microns (μm) deposit mainly in the upper respiratory system while particles that reach the lower parts of the lungs are predominantly between 1 and 3 microns (Figure 1). Below 0.4 microns, particles are diffused into the body.

Indoor concentrations of fine particles were determined in 48 homes in Australia (Stratico and Dingle, 1996). Three monitoring sites were chosen in each home, i.e. living room, bedroom and dining room. The combined average of monitoring at all sites gave a 2 hour $PM_{2.5}$ concentration of 34.4 μg/m^3. In the prese modelling work, particle sizes (aerodynamic diar eters) from 0.5 to 6 microns have been investigate This particle range is assumed to be the cause of mar occupational health and indoor environment problem

A significant feature of these particle-laden flow and notably the major stumbling block preventi their detailed solution and our full physical unde standing of them, is the presence of a very wide spe trum of important length and time scales (Elghobash 1994). Understanding of the turbulence in particle-fr flows is still incomplete. This sets an upper limit to t current understanding of the more complex particl laden turbulent flows. For low particle concentratio there is, however, a negligible effect on turbulence (s Figure 2). Here the interaction between particles ar turbulence is termed one-way coupling. The partic dispersion then depends on the state of air turbulen but, due to a low concentration of the particles, t momentum transfer from the particles to the turb lence has an insignificant effect on the flow.

Existing Approaches of Particle-Laden Flow Modelling

Two different mathematical treatments of partic movements in airstreams are possible. One deals wi the fluid phase as a continuum and the particula phase as single particles. This is the Lagrangian a

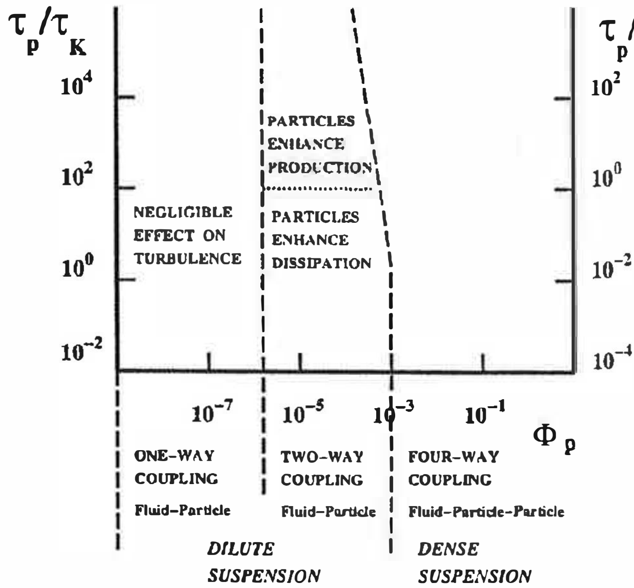

Fig. 2 Regimes of fluid-particle interaction, where Φ_p is the v ume fraction of particles, τ_p is the particle response time, τ_k is Kolmogorow time scale, and τ is the turnover time of large edd (Elghobashi, 1994)

proach. Particle trajectories are predicted as a result of forces acting on the particles. The particle dispersion must be incorporated through an empirical diffusion velocity or more accurate Monte Carlo methods (Mostafa and Mongia, 1987; Crowe, 1982). An alternative approach using velocity probability density functions to describe particle dispersion in turbulent flows is suggested by Lockwood (1989). A Lagrangian computational model for simulating particle dispersion and deposition in the human tracheobronchial tree is suggested by Li and Ahmadi (1995). In this model, the instantaneous turbulence fluctuating velocity is simulated as a continuous Gaussian random vector field. Large particles, e.g. particles generated from grinding wheels, are normally modelled by Lagrangian models (Alenius and Johansson, 1996).

The other approach, the Eulerian approach, treats the solid particles as a continuum. The appropriate transport (continuum) equations for the bearing fluid and the particles are solved respectively. Normally this means that the governing equations are similar to the Navier-Stokes equations with some extra source/sink terms. To be able to use the Eulerian approach for particle dispersion, some kind of continuum criteria must be justified. Continuum criteria are discussed by Batchelor (1974) and Lumley (1978). For this approach to be valid, each computational element should contain a number of particles so that statistically averaged properties can be assumed for the particles. Also, the particle size should be significantly smaller than the Kolmogorow microscale, η.

The parameters governing the micro length scale include the dissipation rate per unit mass, ε, and the kinematic viscosity, ν. For the Kolmogorow length scale, η, Etheridge and Sandberg (1996) give:

$$\eta = \left(\frac{\nu^3}{\varepsilon}\right)^{0{,}25} \qquad (1)$$

For a ventilated room, the dissipation rate was experimentally estimated by Etheridge and Sandberg (1996), at a value of about 1 mm for the micro length scale. The largest particle diameters used in our examples were 0.5 per cent of the micro length scale.

In Mostafa and Mongia (1987) a lot of research work is mentioned where Eulerian approaches have been used to predict two-phase flows.

Model Used for the Present Work

Low-particle volume fractions with relatively small particle diameters are arguments for treating the particles as a continuum. A drift-flux multi-phase model has been chosen rather than a fully coupled multi-fluid model. In previous investigations, drift-flux models have been successfully used to study settling tanks and clarifiers (Celik and Rodi, 1989; Adams and Rodi, 1990; Zhou and McCorquodale, 1992). Li and Rudman (1997) used a drift-flux model for particle separation in a bottom-feed separation vessel. A fully two-phase model was compared to the drift-flux model and for a free-settling problem with low solid loadings almost identical results were obtained. Murakami et al. (1992) applied the drift-flux model in a clean room.

A main advantage of the drift-flux model used here is that a number of different particle sizes can be included in the model. This would have been computationally prohibitive with a fully multi-phase treatment.

Governing Equations

The governing equations are given in vector form:

$$\nabla \cdot (\rho \boldsymbol{V}) = 0 \qquad (2)$$

$$\frac{\partial(\rho \boldsymbol{V})}{\partial t} + \nabla \cdot (\rho \boldsymbol{V} \otimes \boldsymbol{V}) = \nabla \cdot (\mu_{eff} \nabla \boldsymbol{V}) - \nabla \boldsymbol{P} + \boldsymbol{f} \qquad (3)$$

$$\frac{\partial(\rho \Phi)}{\partial t} + \nabla \cdot (\rho \boldsymbol{V} \Phi) = \nabla \cdot \left(\frac{\mu_{eff}}{\sigma_\Phi} \nabla \Phi\right) + S_\Phi \qquad (4)$$

$$\frac{\partial(\rho C_i)}{\partial t} + \nabla \cdot (\rho(\boldsymbol{V} + \boldsymbol{V}_s) C_i) = \nabla \cdot \left(\frac{\mu_{eff}}{\sigma_{C_i}} \nabla C_i\right) + S_{C_i} \qquad (5)$$

where **V**, **P** and $\boldsymbol{V}_s$ are the velocity vector, pressure and settling velocity vector respectively. C_i is the volume concentration of particle class *i*. The effective viscosity μ_{eff} is the sum of molecular and turbulent viscosity, and the density is ρ. The body force *f* due to particle/fluid density differences is modelled by using a Boussinesq approximation. Turbulence is modelled using a standard κ-ε model with wall functions applied at near wall surfaces. So Φ in Equation (4) can be κ or ε and the non-dimensional numbers σ_Φ (1.0) and σ_{Ci} (1.0), in Equations 4 and 5, represent the turbulent diffusivity of Φ and C_i, respectively. The effect of particles on turbulence has not been considered in the current study as it is believed that the low solids loadings and comparatively small particle settling velocities have only a very small effect when compared to the high inflow turbulence levels. It is also assumed that the particle size distribution will not be altered by coagulation due to low solids loadings in this study. The possible influence of the body force *f* on κ and ε is not considered.

All variables are defined at the supply inlet. A zero-gradient condition is applied at the outlets and the airflow rates are distributed with a predetermined ratio through the outlets. A finite volume technique based on the SIMPLEC algorithm was used to solve the time-averaged multi-phase Navier-Stokes equations. The convection terms in the momentum equations are discretized using a second-order finite volume scheme (QUICK) for non-uniform grids (Li and Baldacchino, 1995). A first-order upwind scheme is used for solid-fraction equations and the governing equations for turbulence kinetic energy and its dissipation rate.

Discretization of the Solid Particle Equation

There are several ways to incorporate Equation (5) into the SIMPLEC algorithm. One way is to rearrange Equation (5) as:

$$\frac{\partial(\rho C_i)}{\partial t}+\nabla\cdot(\rho \boldsymbol{V} C_i)=\nabla\cdot\left(\frac{\mu_{eff}}{\sigma_{C_i}}\nabla C_i\right)+S_{C_i}-\nabla\cdot(\rho \boldsymbol{V}_s C_i) \tag{6}$$

The last term on the right-hand side represents a settling effect and is treated as a source term in the discretized equation.

The approach used here is to discretize Equation (5) directly and include the settling velocity in the convection term. Note that the velocity field ($\boldsymbol{V}+\boldsymbol{V}_s$) is not divergence-free, so a continuity equation cannot be used in the discretization of the convection/diffusion equation, as is normally done, e.g. Patankar (1980).

In Patankar's SIMPLE approach, the following discretization equation is obtained for particle concentrations:

$$a_P C_P=\sum_{nb=1}^{N} a_{nb} C_{nb}+c_o \tag{7}$$

where P represents the cell centre and nb the neighbouring points. The number of neighbouring points N, the coefficients a_P, a_nb and the source term c_o of the discretization equation depend on the discretization schemes used. When the flow field is required to satisfy the continuity equation, the descretized continuity equation can be used to ensure the following desirable property in the discretization equation:

$$a_P=\sum_{nb=1}^{N} a_{nb} \tag{8}$$

With the governing equations for particle concentrations in the drift-flux model, the particle flow field does not satisfy the continuity equation, and the above property will not need to be ensured.

Settling and Deposition – Boundary Conditions

The settling velocity of a particle is derived by equalling the fluid drag force on the particle (given by Stokes equation) with the gravitational force on the particle. It is a velocity relative to air under steady-state conditions. It equals the product of the acceleration due to gravity and the relaxation time of the ticle.

Important parameters in particle deposition mation include particle-size-dependent diffusivity surface-to-air temperature differences. Equations Nazaroff and Cass (1989), suitable for indoor air lutants, do not include particle inertia because of air velocities in indoor airflows.

When particles are dispersed in air, the ranc movement will always result in a net transport wards areas of lower concentration, and the drift ocity is proportional to the gradient of the pollu concentration (Lange, 1995). Deposition to solid faces can thus, in a simplified approach, be contro by giving different boundary conditions for the par concentration at the wall C_w. A turbulent diffus controlled deposition is established by assuming:

- $C_w=0$; maximum deposition to the wall
- $\partial C/\partial n=0$; no deposition to the wall; zero nor gradient.

In the present paper we assume for deposition by fusion:

- $C_w=\alpha C_{nw}$, where $0\leq\alpha\leq 1$.

C_{nw} is the first normal grid point concentration. Th an empirical approach where appropriate α-values be found from measured deposition values. Unfo nately, the value of α is grid-dependent. It is propo here to demonstrate the particle deposition effect, an effective deposition boundary condition needs t developed.

It is expected (Eaton, 1994) that single-phase tu lence models will overestimate turbulence level particle-laden flows. For the indoor pollutants stu here, the mass loading ratio is very small and t effects are assumed negligible. The turbulence atte ation is apparently affected by several parameters cluding the particle Stokes number, the Reynolds n ber, and possibly the ratio of the particle diameter a length scale of the turbulence. Also, there are di ences in the turbulence attenuation between bounded and homogeneous turbulent flows.

Evaluation and Applications

An Aerosol Chamber Simulation

Results from measurements with turbulent flow ditions and a sensitive aerosol detection techni Byrne et al. (1995), have been used for validating numerical calculations of particle movements in investigation. An aluminium cube test chamber m^3, where turbulent flow conditions were genera

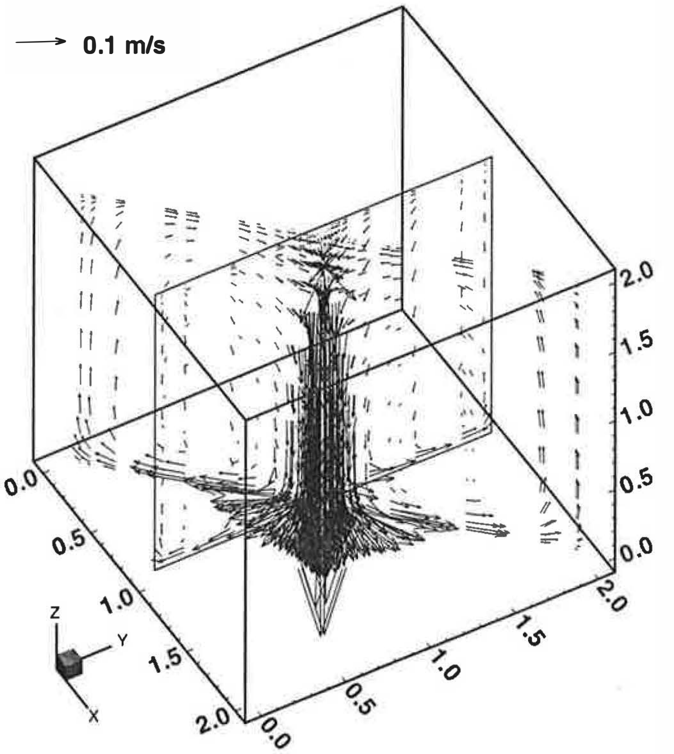

Fig. 3 The velocity field at the centerline and diagonal planes in the aerosol chamber

with a rotating fan, was used for the measurements. Air velocities, turbulence levels and average aerosol deposition velocities on all surfaces were measured for particles of different mono-disperse particle sizes. Aerodynamic diameter is used to represent the particle sizes in this paper. The numerical simulations were designed to follow the experimental work fully, while a model of a fully equipped chamber was set up in three dimensions. Figures 3–5 show the geometry and the general air and particle flow patterns in the test chamber generated by the ceiling fan. The velocity profile generated by the ceiling fan at the fan exit was measured and is used here as the boundary condition for the simulation. The figures are based on transient calculations showing the results 15 minutes after the settling process was started. The flow pattern agrees well with the measured flow pattern presented in Byrne et al. (1995).

The non-uniform grid used is 20×20×20. A finer grid of 40×40×40 produced similar velocity fields. No grid-independent test was done for the particle deposition, as the deposition boundary condition used here is itself grid-dependent.

The simplified deposition model presented earlier was demonstrated in the numerical simulations. Two particle sizes were considered: 2.5 µm with an initial concentration of 31.7 mg/m^3 and 4.5 µm with an initial concentration of 55.3 mg/m^3. The particles were transported through boundaries, and deposition velocities were compared to experiments in the test chamber

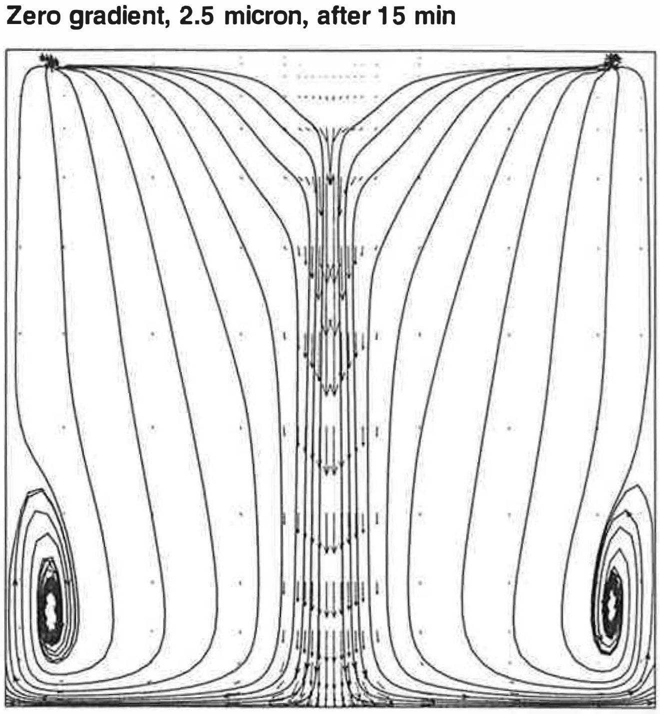

Fig. 4 The velocity field and streamlines at the centerline plane in the aerosol chamber under equivalent conditions as in Figure 3

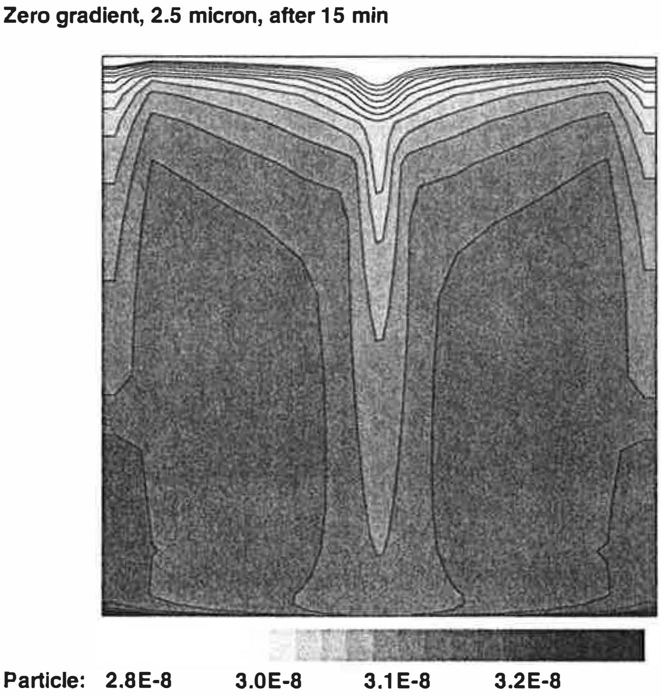

Fig. 5 Distribution of volume fractions at the centerline plane in the test chamber. The model includes wall settling but no deposition on the walls or ceiling. No mass transport is allowed through the boundaries

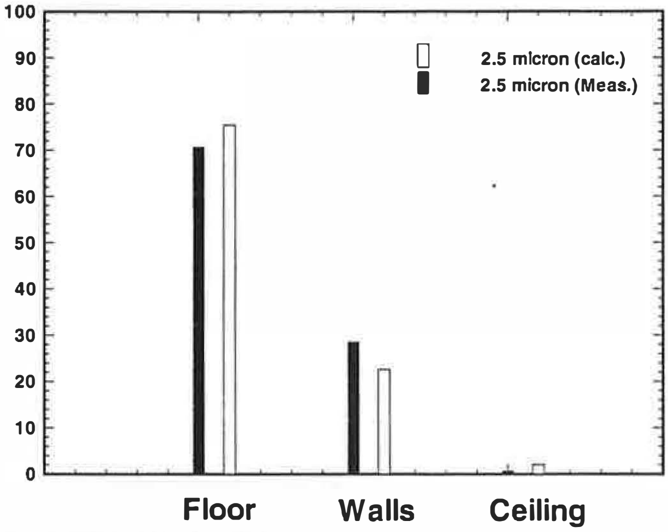

Fig. 6 Comparison of predicted and measured relative deposited particle mass at floor, ceiling and vertical wall with 2.5 µm (aerodynamic diameter) particles

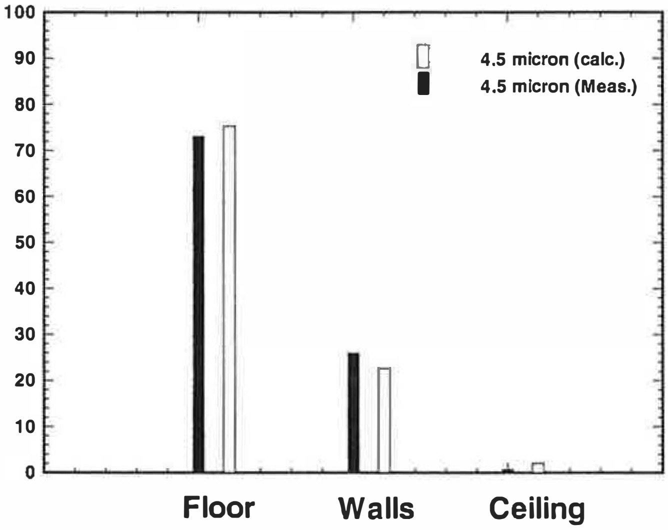

Fig. 7 Comparison of predicted and measured relative deposited particle mass at floor, ceiling and vertical wall with 4.5 µm (aerodynamic diameter) particles

where real deposition occurred. Thus, no resuspension of deposited particles was possible. The results are shown in Figures 6 and 7. The agreement is generally good. However, it should be mentioned that the results shown in the two figures were obtained by tuning the values of α for different surfaces for the grid used in the simulation. The final tuned α values are 0.95, 0.995 and 0.67 for walls, floor and ceiling respectively for the 2.5 µm particle case. The final tuned α values are 0.9, 0.99 and 0.65 for walls, floor and ceiling respectively for the 4.5 µm particle case. The comparison can only be considered as representative. A better and physically sensible deposition boundary condition is
needed. In a ventilated room, the particle trans
process is generally controlled by particle disper
due to convection. Examples are given below.

Particle Dispersion in a Ventilated Room

In this example, a high-velocity mixing ventilation
was tested. This particular example could be a c
room or other room where many air changes ar
quired. A 10 ppm particle concentration was supp
with the incoming air. The geometry of the room
the airflow condition are shown in Figure 8. The
area under the ceiling is 1.5×0.5 m^2 and the outlet
from the floor level is 1.5×1 m^2. A 32×22×22 grid
used for the isothermal calculations. The particle d
sition through boundaries was not considered in
example.

These calculations were carried out with diffe
mono-disperse particle sizes in a realistic ventila
application. A 10 ppm particle concentration was
plied to the room with the incoming ventilation
flow. The calculations show a strong dependenc
particle diameter. Particles tested in our investiga
ranged from 5 µm to 0.5 µm. It can be seen in Figu
that smaller particles tend to be uniformly distrib
in this almost fully mixed room, while larger part
tend to settle in the lower (low velocity) part o
room.

Particle Flow near a Person

Brohus and Nielsen (1996) presented different
models of a person and evaluated them by compar
with full-scale measurements. For this purpose a
mal manikin, standing in a wind channel, was use
laboratory experiments. The spread of locally ge

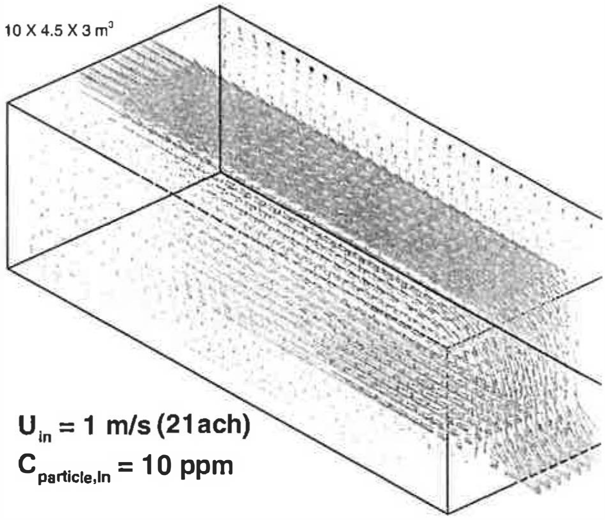

Fig. 8 Geometry of the room and the flow condition for p
dispersion in a ventilated room

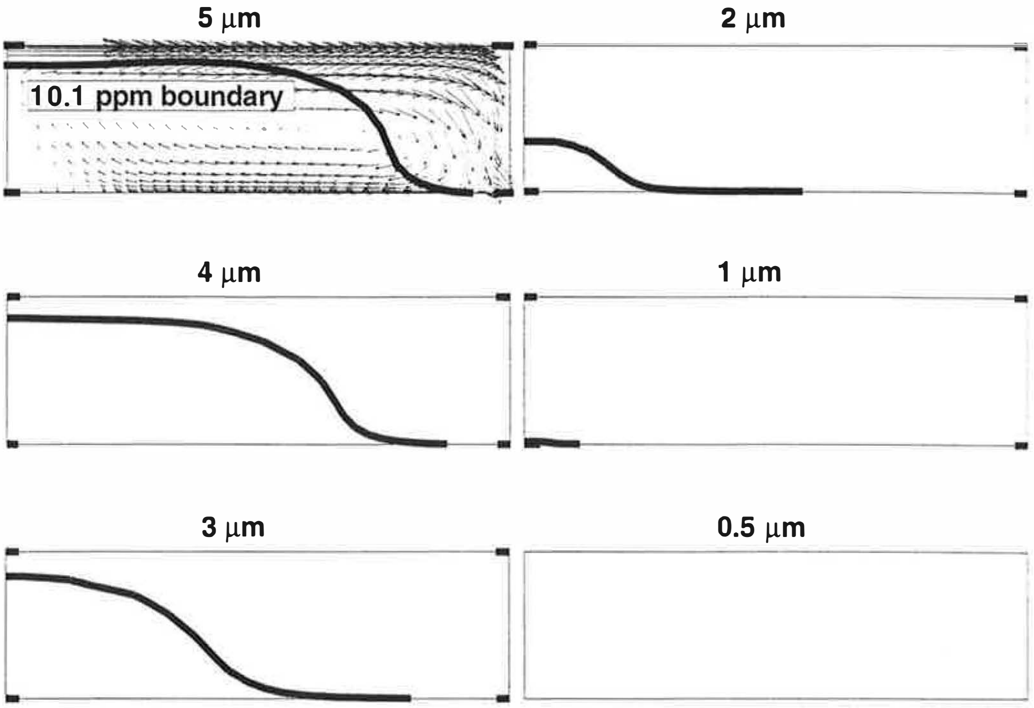

Fig. 9 Particle concentrations at the centerline plane for different particle sizes. The area under the black line shows increased room concentrations, i.e. the boundary for room concentrations greater than 10.1 ppm. With a small particle size this area is negligible

ated passive contaminants in the near field of the manikin was compared to numerical experiments. One aim of the experiments was to find out whether the turbulent flow conditions generated downstream of the manikin would be able to bring the locally generated contaminants up into the breathing zone. In the present work, a similar investigation based on numerical calculations was made using non-passive contaminants which therefore were expected to behave differently from the passive contaminants used by Brohus and Nielsen. In the centre plane, 1 m from the floor level and 0.45 m from the manikin, a particle cloud with a mono-disperse aerodynamic diameter distribution of 5.0 µm was locally generated in the particle source (Figure 10). The volumetric source strength was 5.8×10^{-6} m^3/s. A non-uniform grid of 42×22×41 was used.

The thermal manikin comprised three different body segments. Each of them could easily be equipped with unique thermal data. For this case, however, we used a constant convective heat flux of 25 W/m^2 for all segments. The total surface area of the manikin was 1.65 m^2. The convective heat plume generated by the manikin, streamlines of incoming air and velocity vectors around the thermal manikin are shown in Figure 11. With experience from the work by Brohus and Nielsen (1996), one can expect that the thermal plume around the manikin, in combination with recirculating turbulent air, would be able to bring contaminants into the breathing zone. The airflow between the manikin legs is important for the spread of the particles from the local source. The temperature of the incoming air was 21°C.

According to the simulated results, shown in Figure 12, the particle cloud does not impinge into the convective plume flow surrounding the manikin, and the

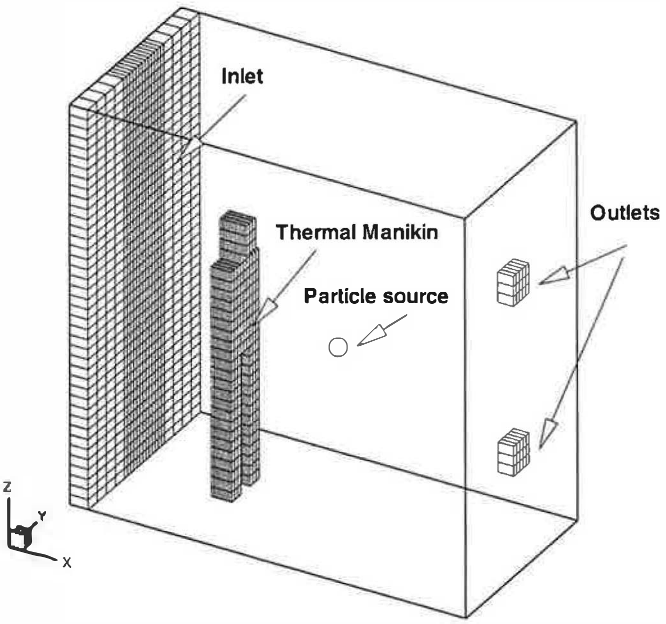

Fig. 10 Geometry of the test room and the thermal manikin used in the numerical simulations. The whole inlet wall was open for air supply. The influence of recirculation effects downstream of the thermal manikin on the spread of the contaminants from the local source was investigated

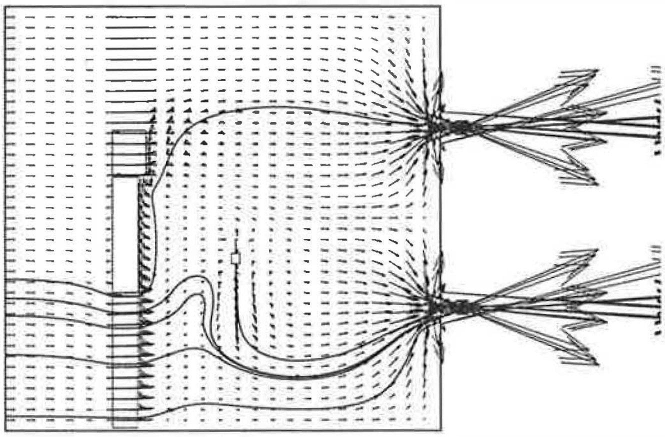

Fig. 11 Central x-z cut showing thermal manikin with surrounding velocity vectors and streamlines. A uniform free stream supply velocity of 0.3 m/s from the entire supply wall was used. The square in the middle is the particle source

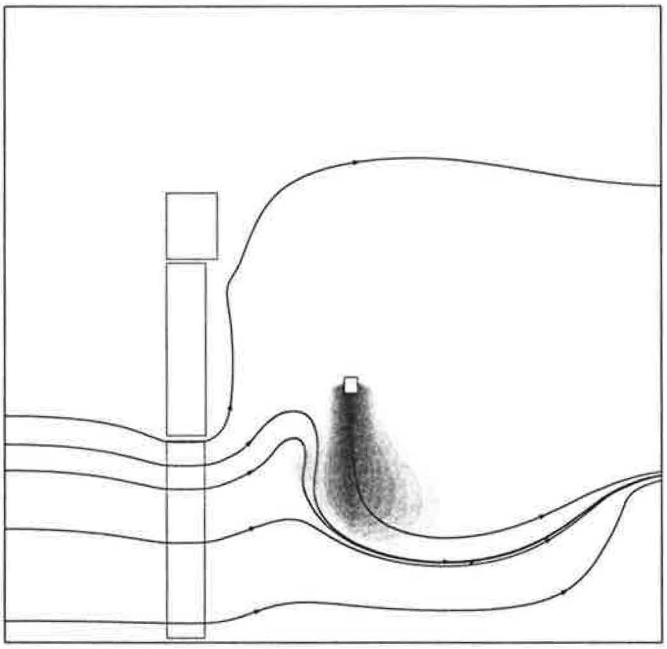

Fig. 12 Streamlines and particle spreading behind (downstream) the thermal manikin. The uniform supply velocity was 0.3 m/s and the particle aerodynamic diameter 5 μm

breathing zone of the manikin remains clean. Brohus and Nielsen (1996) had, for a similar case, the opposite experience with a passive contaminant source (see Figure 13). The upstream diffusion of the particle cloud was here much stronger and the breathing zone was highly contaminated by the local point source.

After decreasing the uniform velocity supply rate from 0.3 m/s to 0.15 m/s the non-passive particle experiment shown in Figures 11 and 12 was repeated. This time the particle settling velocity became rather dominant and the incoming air front was almost stopped by the settling particles (Figures 14 and 15).

According to our numerical predictions, the p
ability of having a contaminated breathing zone
decreased with the lower air supply flow rate of
m/s. The particle size used in this study was 5.0
A smaller particle size would give a lower settling
ocity. Ultra small particles are supposed to behave
proximately as passive contaminants shown in Fi
13. The airflow behaviour is locally (close to the so
in Figure 11) influenced by the particle source stren

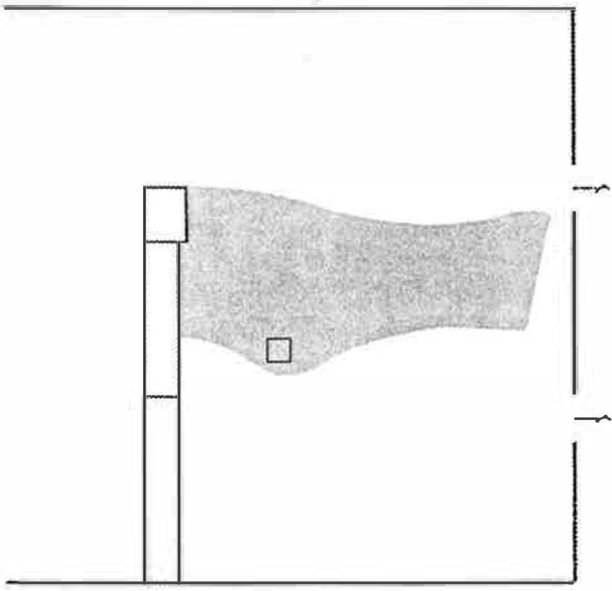

Fig. 13 With passive contaminants, which fully follow the v
lation airstream, a high contaminant concentration is predict
the breathing zone. Numerical simulations by Brohus and
sen (1996). Boundary conditions here are similar to those in
ure 14, with the exception of the non-passive contaminants
there

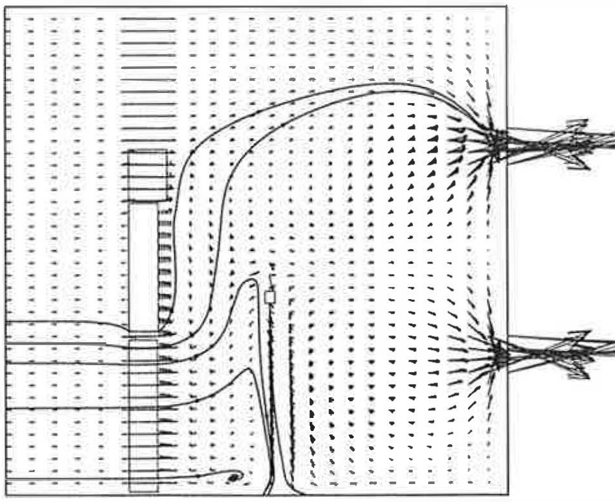

Fig. 14 Central x-z cut showing thermal manikin with surro
ing velocity vectors and streamlines. A uniform free stream
ply velocity of 0.15 m/s from the entire supply wall was
The velocity field below the local particle source is influence
the particle settling

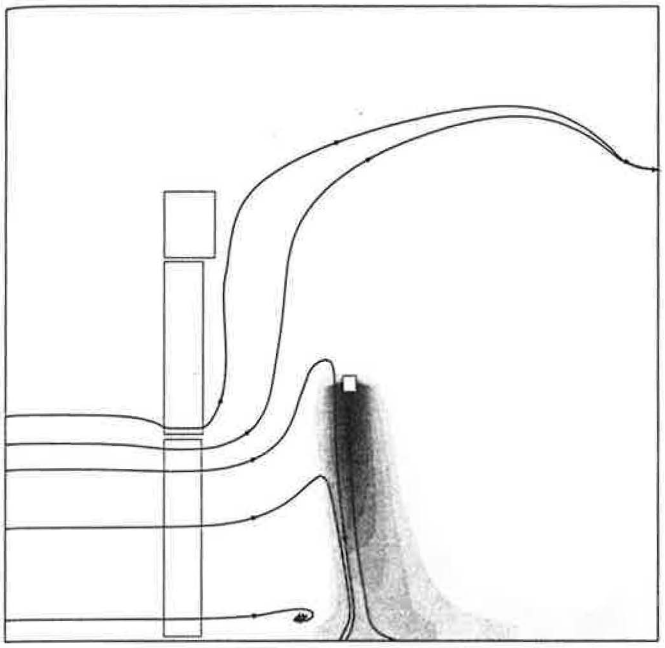

Fig. 15 Streamlines and particle spreading behind (downstream) the thermal manikin. The uniform supply velocity was 0.15 m/s and the particle aerodynamic diameter 5 μm. Particles are forced downstream by the airflow and gravity settling. The breathing zone is not influenced

In such regions, the low particle loading assumption for turbulence modelling may not always be satisfied.

Conclusions and Future Work

An Eulerian-based particle simulation model has been used to simulate dispersion and deposition of particles in the air, which are relevant for indoor environments. Aerosol chamber measurements have been used to check the numerical simulations for two different mono-disperse particle distributions. In the present work, the focus has been on particle dispersion, while particle deposition has only been touched upon to satisfy simple wall boundary conditions for mass transport at solid boundaries. Example simulations of particle-laden flows in realistic indoor environments with different types of mechanical ventilation system have shown that the simulation model can be useful in evaluating designs for reducing particle exposures. It can be used to predict exposure levels at workplaces and in other indoor environments. An improved understanding and better control of indoor pollution sources and pollution movements are important in the sense that control techniques can be implemented to reduce damaging health effects and soiling problems.

The present investigation shows that the deposition on indoor surfaces plays a significant role in the total pollutant balance in indoor environments when the ventilation flow rate is low or when there is no ventilation. It is therefore of great interest and importance in the future to develop deposition boundary conditions which are based on accurate physical laws of airflow and particle movements in indoor environments.

Acknowledgments

This work was carried out when the first author undertook his collaborative research at CSIRO, Australia. The first author would like to thank Dr Jeff Symons and his project team for their hospitality, help, and the stimulating research environment during the author's stay at CSIRO. The visit was sponsored by a scholarship from the Swedish Council for Work Life Research, which is gratefully acknowledged. The authors would like to thank Dr Miriam Byrne at Imperial College in London, who kindly provided the measurement data for this project.

References

Adams, E.W. and Rodi, W. (1990) "Modelling flow and mixing in sedimentation tanks", *Journal of Hydraulic Engineering,* **116**, 895–913.

Alenius, S. and Johansson, J. (1996) "Air flow and particle distribution around a rotating grinding wheel", *Aerosol Science and Technology*, **25**, 121–133.

Batchelor, G.K. (1974) "Transport properties of two-phase materials with random structure", *Journal of Fluid Mechanics.,* **6**, 227–255.

Brohus, H. and Nielsen, P.V. (1996) "CFD models of persons evaluated by full-scale wind channel experiments". In: *Proceedings of Roomvent '96*, Yokohama, 5th International Conference, Vol. 2, pp. 137–144.

Byrne, M.A., Goddard, A.J.H., Lange C. and Roed, J. (1995) "Stable tracer aerosol deposition measurements in a test chamber", *Journal of Aerosol Science*, **26** (4), 645–653.

Celik, I. and Rodi, W. (1989) "Modelling suspended sediment transport in nonequilibrium situations", *Journal of Hydraulic Engineering,* **114**, 1157–1191.

Crowe, C.T. (1982) "Review – numerical models for dilute gas-particle flows", *ASME Journal of Fluid Engineering,* **104**, 297–303.

Eaton, K.J. (1994) *Experiments and Simulations on Turbulence Modification by Dispersed Particles*, American Society of Mechanical Engineers (ASME Reprint No AMR146).

Elghobashi, S. (1994) "On predicting particle-laden turbulent flows", *Applied Scientific Research*, **52**, 309–329.

Etheridge, D. and Sandberg, M. (1996) *Building Ventilation: Theory and Measurement*, Chichester, John Wiley & Sons.

Lange, C. (1995) *Indoor Deposition and the Protective Effect of Houses against Airborne Pollution*", Risø National Laboratory, Denmark (Ph. D. thesis, Risø-R780(EN).

Li, A. and Ahmadi, G. (1995) "Computer simulation of particle deposition in the upper tracheobronchial tree", *Aerosol Science and Technology*, **23**, 201–223.

Li, Y. and Baldacchino, L. (1995) "Implementation of some higher-order convection schemes on non-uniform grids", *International Journal of Numerical Methods in Fluids,* **21**, 1201.

Li, Y. and Rudman, M.J. (1997) "Particle transport in a bottom-feed separation vessel". In: *Proceedings of CFD in Minerals & Metals Processing and Power Generation,* Melbourne.

Lockwood, F.C. (1989) "A new method for the computation of particle dispersion in turbulent two-phase flows", *Combustion and Flame,* **76**, 403–413.

Lumley, J. L. (1978) "Two-phase and non-Newtonian flows". In: Bradshaw, P. (ed.) *Turbulence,* Berlin, Springer, p. 289.

Mostafa, A.A. and Mongia, H.C. (1987) "On the modelling of turbulent evaporating sprays: Eulerian versus Lagrangian approach", *International Journal of Heat and Mass Transfer,* **30** (12), 2583–2593.

Murakami, S., Kato, S., Nagano, S. and Tanaka, Y. (1992) "Diffusion characteristics of airborne particles with gravitational settling in a convection-dominant indoor flow field", *ASHRAE Transactions,* **98**, Pt. 1, 82–97.

Nazaroff, W.W. and Cass, G.R. (1989) "Mathematical modelling of indoor aerosol dynamics", *Environm Science and Technology,* **23**, 2.

Owen, M. K., Ensor, D.S. and Sparks, L.E. (1992) "Airb particle sizes and sources found in indoor air", *Atmosp Environment,* **26A** (12), 2149–2162.

Patankar, S.V. (1980) *Numerical Heat Transfer and Fluid* New York, McGraw-Hill Book Company.

Stratico, A. and Dingle, P. (1996) "Background fine partic levels in Australian homes". In: *Proceedings of Indoor A* Nagoya, 7th International Conference on Indoor Air ity and Climate, Vol. 1, pp. 591–594.

Wickham, F. (ed.) (1992) *Air Filters,* Australia, AIRH (No 15).

Zhou, S. and McCorquodale, J.A. (1992) "Modelling of tangular settling tanks", *Journal of Hydraulic Engine* **118**, 1391–1405.